CIMAC CONGRESS 25
ZURICH, MAY 19 – 23, 2025

2025 | 009

Combustion Characteristics of a Dual-Fuel Marine Engine with Different Methanol Substitution Rate

Dual Fuel / Gas / Diesel

Xiao Li, National Key Laboratory of Marine Engine Science and Technology, Shanghai Marine Diesel Engine Research Institute

Ping Yan, Shanghai Marine Diesel Engine Research Institute
Yuqi Jiang, National Key Laboratory of Marine Engine Science and Technology, Shanghai Marine Diesel Engine Research Institute
Hongmei Li, National Key Laboratory of Marine Engine Science and Technology, Shanghai Marine Diesel Engine Research Institute
Liang Zheng, National Key Laboratory of Marine Engine Science and Technology, Shanghai Marine Diesel Engine Research Institute
Lijun Guo, Shanghai Marine Diesel Engine Research Institute
Wenzheng Zhang, National Key Laboratory of Marine Engine Science and Technology, Shanghai Marine Diesel Engine Research Institute
Chao Chen, National Key Laboratory of Marine Engine Science and Technology, Shanghai Marine Diesel Engine Research Institute

---

This paper has been presented and published at the 31st CIMAC World Congress 2025 in Zürich, Switzerland. The CIMAC Congress is held every three years, each time in a different member country. The Congress program centres around the presentation of Technical Papers on engine research and development, application engineering on the original equipment side and engine operation and maintenance on the end-user side. The themes of the 2025 event included Digitalization & Connectivity for different applications, System Integration & Hybridization, Electrification & Fuel Cells Development, Emission Reduction Technologies, Conventional and New Fuels, Dual Fuel Engines, Lubricants, Product Development of Gas and Diesel Engines, Components & Tribology, Turbochargers, Controls & Automation, Engine Thermondynamis, Simulation Technologies as well as Basic Research & Advanced Engineering. The copyright of this paper is with CIMAC. For further information please visit https://www.cimac.com.

ABSTRACT

Methanol is a suitable alternative fuel to relieve the problem of energy shortage and decrease the emission of greenhouse gases. The effect of methanol substitution rate (MSR) on the combustion and emission characteristics of a marine diesel-methanol double direct-injection engine with bore of 210 mm was simulated with a 3-dimentional computational fluid dynamic (CFD) software AVL-FIRE. The combustion model was set-up and validated by the experimental data from the marine diesel engine. Results show that the increased MSR results in the decreasing of the first peak value of heat release rate and the increasing of the second peak value of heat release rate. With the increase of MSR, the ignition timing advances, the combustion duration shortens gradually, indicated mean effective pressure and thermal efficiency increase. At the load of 25%ï¼Œthe emissions of nitrogen oxide and soot reduce with increased MSR. At the load of 100%, the emissions of nitrogen oxide and soot first decrease and then increase. At a low load condition, the MSR must be maintained at a high level to decrease the emission of nitrogen oxide. However, a suitable range of MSR can ensure the output of engine power and make emissions under a low level simultaneously at high loads.

1 INTRODUCTION

The energy shortage, environment pollution and global warming are becoming more and more serious in recent years. The global carbon dioxide (CO_2) emissions need to be reduced urgently. Representative agreements such as United Nations Framework Convention on Climate Change, Kyoto Protocol, and Paris Agreement, has been signed, outlining the goals and directions for global climate governance and carbon emission reduction [1]. In China, “Carbon Peaking” and “Carbon Neutrality” should be attained in 2030 and 2060, respectively [2]. The diesel engine has been used to provide power for the propulsion of marine or as a power generation unit on the ship due to its high efficiency, durability, and reliability [3]. In 2018, the International Maritime Organization (IMO) proclaimed the initial IMO strategy on reduction of greenhouse gas (GHG) emissions from ships. In this strategy, a reduction in carbon intensity of international shipping (to reduce CO_2 emissions per transport work, as an average across international shipping, by at least 40% by 2030, pursuing efforts towards 70% by 2050, compared to 2008) needs to be realized; and that total annual GHG emissions from international shipping should be reduced by at least 50% by 2050 compared to 2008 [4]. Hence, the CO_2 emission from marine diesel engine needs to be reduced urgently. In the meantime, a mass of soot and NO_X are produced during the diffusive combustion of diesel due to the existence of local high temperature and rich region during the combustion process [5].

Applying alternative fuel on the marine diesel engine is one of effective methods to attain the “Carbon Peaking” and “Carbon Neutrality” and reduce NO_X and soot emissions. The alternative fuels used on marine diesel engine are natural gas [6], methanol [7], ammonia [8] and hydrogen [9], etc. Methanol as an alternative fuel can achieve smokeless combustion due to the high oxygen content and no carbon-carbon bond [10]. Simultaneously, its property of higher laminar flame velocity as compared with diesel is conducive to improving thermal efficiency [11]. Several methods such as fuel blends [12], methanol fumigation [13], part premixed and non-premixed dual-fuel [14, 15] have been applied on the diesel engine to organize the combustion of methanol. The fuel blends method [16] needs additive to promote the mixing of methanol and diesel, in which fuel stratification is easy to occur. The methanol blend ratio is lower than other methods and cannot be changed with operation conditions. Yao et al. [17] investigated the effect of methanol fumigation on a turbocharged inter-cooling diesel engine. They found that the carbon monoxide (CO), hydrocarbon (HC) emissions were increased but NOx and soot emissions were significantly reduced. By using methanol fumigation method, the max methanol substitution percentage (MSP) is 80% with both high pressure (HP) and low pressure (LP) exhaust gas recirculation (EGR) system [18]. The NO_X and PM emissions levels meets the China VI emission legislation [19]. Jia et al. [14] studied the part premixed methanol-diesel direct-injection (DI) dual-fuel combustion characteristics on a heavy-duty engine. In this method, the DI timing of methanol is earlier than that of diesel. They found that the max MSP can be 76.3% with IMEP at 12 bar and EGR at 39%. This application of this method cannot be extended to the high load. Dong et al. [15] investigated non-premixed methanol-diesel DI dual-fuel engine concept on a single-cylinder dual-fuel engine. They found that the MSP can be higher than 90% at high load with low cycle-to-cycle variation of IMEP, ultra-low emissions and high thermal efficiency. In this method, the DI timing of methanol is later than that of diesel. The combustion in the cylinder under this mode is diffusive combustion. Hence, the combustion is stable. MAN and Wärtsilä [20,21] applied this combustion mode on their marine diesel engines with bore of 350 mm and 320 mm, respectively. The total excess air ratio is around 2.0. However, other detail about combustion cannot be found. According to the previous researches, the range of excess air ratio for methanol combustion is extensive [22, 23]. But the range of excess air ratio for stable combustion with low emissions cannot be found. This method has some advantages as followed [24]: It can avoid the occurrence of incomplete combustion at low load and the crude combustion at high load; It can control the injection mass of methanol in every cylinder with high precision and decreasing the unevenness of cylinders; It can avoid the scavenging of methanol mixture during the valve overlap; It can maintain the volumetric efficiency at a same level as original diesel engine and power output; The MSP can be higher than 90% and emissions are ultra-low under this mode. Hence, non-premixed methanol-diesel DI dual-fuel engine concept is suitable for diesel engine.

As described above, the characteristics of methanol/diesel dual-fuel non-premixed combustion with large bore marine engine are not clear. In order to design a methanol/diesel dual-fuel non-premixed combustion engine, it is necessary to take a deeper insight into the effect of operating parameters on the combustion and emissions characteristics. Hence, the effects of the methanol substitution rate (MSR) equivalence ratio, temperature distribution, combustion and

emission characteristics are simulated on a marine diesel engine with bore of 210 mm.

2 NUMERICAL SETUP

2.1 Meshing and Modeling

Three-dimensional simulations were performed with the AVL FIRE™ software. The simulation process was carried out on a marine diesel engine. Table 1 shows the specifications of the marine diesel engine. 0°CA is defined as the combustion top dead center (TDC) in this study. The simulation domain is from intake valve closing (IVC) to exhaust valve opening (EVO). The diesel is surrogated by n-decane, methylbenzene, methyl cyclohexane and iso-octane with volume fraction of 59.48, 20.03, 10.48 and 10.01% respectively. Since the nozzle number of methanol and diesel injector is 10, a one-tenth combustion chamber model, showed in Figure 1 is established.

The meshes was generated by the ESED module in AVL FIRE as shown in Figure 2. The base grid size of the combustion chamber is 2 mm. To maintain the computational accuracy during spray process, the meshes around injector and spray zone are refined based on the distribution of methanol and diesel spray showed in Figure 3. In Figure 3, the blue and orange zone are used to represent methanol and diesel spray, respectively.

RANS based on realizable k-ε turbulence model is used to calculate the flow field in the cylinder, which solves the turbulent vortex and viscidity of fluid with low Reynolds number and can improve the computational accuracy near the wall. O'Rourke model was used to calculate the wall heat transfer.

KH-RT model was used to calculate the spray breakup process of methanol and diesel surrogate. In this model, aerodynamic instabilities are responsible for the primary breakup of the liquid parent blobs while the secondary breakup of the child drops is based on the competition of the KH and RT mechanisms. The collisions between fuel droplets were described by NTC model. The fuel wall impingement was calculated by the O'Rourke film splash model. The discrete multi-component model is for each component during fuel vaporization. The spray behavior is modeled by the Lagrangian parcel tracking method.

The GGRP coupled with chemical kinetic mechanism was used to calculate the combustion process of methanol and diesel. A skeletal chemical kinetics mechanism with 73 species and 296 elementary reactions for methanol and diesel surrogate fuel was used to model fuel combustion in the cylinder. To calculated the emission of nitrogen oxides (NO_X) and soot, the extended Zeldovich NOx model and Hiroyasu soot model were coupled to the combustion model.

Table 1. Engine Specifications

Parameters	Value
Bore (mm)	210
Stroke (mm)	320
Number of Valves	4
Sweep Volume (L)	11.3
Geometric Compression ratio	17
Engine Speed (r/min)	1000(100%) 630（25%）
Intake Valve Closing (°CA)	535
Exhaust Valve Opening (°CA)	828
Direct Injection Pressure of Methanol (bar)	600
Nozzle (number× diameter(mm)×cone angle (°))	10×0.69×140
Direct Injection Pressure of Diesel Surrogate (bar)	480
The Mass of Injected Diesel Surrogate per Cycle (mg)	120
Nozzle (number × diameter (mm) ×cone angle (°))	10×0.35×145
Fuel Composition of Diesel Surrogate by Volume	59.48% n-decane, 20.03% methylbenzene, 10.48% methyl cyclohexane and 10.01% iso-octane

Figure 1. Geometric model of combustion chamber

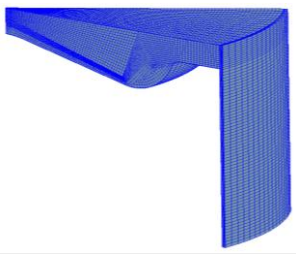

Figure 2. The meshes of combustion chamber

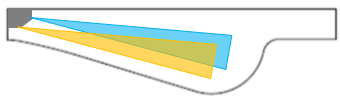

Figure 3. The schematic diagram of the distribution of diesel and methanol Spray

2.2 Simulation Validation

To validate simulation models mentioned above, experiments were carried on the marine diesel engine test bench. The in-cylinder pressure and heat release rate between the experiment and simulation results were validated at diesel mode and diesel-methanol dual-fuel mode, respectively.

During experiments, heat release rate (HRR) was calculated as follows:

$$\frac{dQ}{dt} = \frac{1}{\gamma - 1} \times \left(\frac{Vdp}{d\theta} + \gamma \times \frac{pdV}{d\theta} \right) \quad (1)$$

Figure 5(a) and (b) show the simulation results of in-cylinder pressure and heat release rates. It can be seen that the simulation results are in good agreement with the experiments. It means that the validated models can be used to predict combustion events.

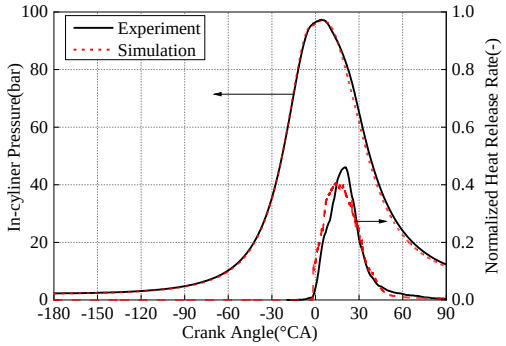

(a) Diesel mode

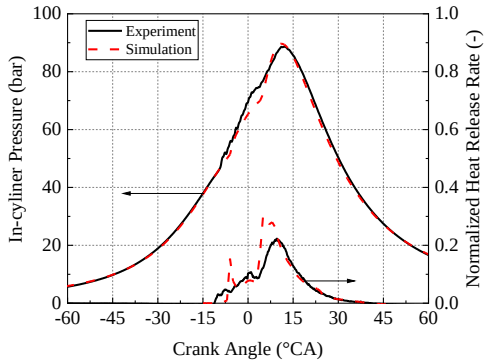

(b) Methanol-Diesel Dual-Fuel mode

Figure 4. Comparison of In-cylinder Pressure and Heat Release Rate between the Experimental and Numerical Results under Different Combustion Modes

2.3 Cases Setup

To understand the effect of methanol substitute rate (MSR) on fuel distribution, combustion and emission characteristics at different load, numerical cases were designed in Table 2. The simulations were carried out between intake valve closing (IVC) and the exhaust valve opening (EVO) in one cycle. In all cases, the initial component in the cylinder was nitrogen and oxygen with the mass fraction of 0.767 and 0.233, respectively. The one-dimensional GT-Power code was used to calculate the initial conditions showed in Table 2. These cases can be divided into two groups to study the effect of MSR on the combustion and emission characteristics by engine load. At different load, the direct injection (DI) timing of diesel surrogate fuel (SOI_D) and methanol (SOI_M) are fixed. During simulation, the mass of injected methanol per cycle is fixed at a certain count at different load. The MSR is changed by changing the mass of injected diesel surrogate per cycle.

Table 2. Numerical Cases

Cases	Load (%)	Initial Tempe--rature (K)	Initial Pressure (bar)	SOI_D (°CA ATDC)	SOI_M (°CA ATDC)	MSR (%)
1						70
2	25	340	1.2	-13	-4.5	77
3						84
4						85
5	100	340	3.4	-10	-1	90
6						95

2.4 Parameter Calculation

The MSR is defined as follows:

$$MSR = \frac{m_M \times LHV_M}{m_D \times LHV_D + m_M \times LHV_M} \quad (2)$$

Where, m_M is the mass of methanol in the direct injection. m_D is the mass of diesel surrogate fuel burned in a cycle. LHV_M and LHV_D are low heat value of methanol and diesel surrogate fuel, which is 19.9 and 42.7 MJ/kg, respectively.

Ignition timing (CA05), CA50 and CA90 are the crank angles at which 5%, 50% and 90% of the energy stored in the fuel in a cycle is released, respectively. Combustion duration is the crank angle between CA05 and CA90.

3 RESULTS AND DISCUSSION

3.1 Distribution of NO_X, Equivalent ratio and Temperature

Figure 5 shows the distribution of NO_X at different MSRs at load of 25%. It can be seen that the area of distribution of NO_X increases with increased MSR when the crank angle is -5 °CA ATDC due to the increased area of high temperature region (Figure 7). However, the mass fraction of NO_X is lower than 0.00105 at different MSRs. The distribution of NO_X extends with crank angle at different MSRs. The area of the distribution of NO_X decreases with increased MSR after the combustion TDC due to decreased area of high temperature region (Figure 7). The in-cylinder temperature can be decreased with the increased MSR due to the evaporation of methanol. Although the region with higher equivalent ratio decreases with increased MSR, the emission of NO_X decreases. Hence, the cooling effect of methanol on the production of NO_X is stronger than that of oxygenation reaction of methanol at 25% load.

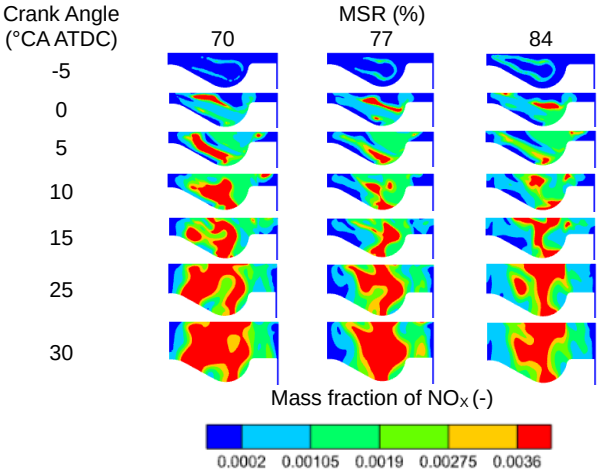

Figure 5. The effect of MSR on the distribution of NO_X at 25% load

Figure 6 shows the distribution of equivalent ratio at different MSRs at load of 25%. It can be seen that spray penetration decreases with the increased MSR when the crank angle is -5°CA ATDC due to decreased mass of diesel before methanol injection. With the injection of methanol, the methanol and diesel spray impinge the piston bowl at combustion TDC. The area of region with equivalent ratio higher than 3.0 decreases with increased MSR due to the enhanced evaporation effect with increased mass of methanol. There is a region with equivalent ratio between 1.75 and 3 around the throat of the piston bowl at all cases. The distance between this region and cylinder wall decreases with increased MSR. After 5 °CA ATDC, the distribution of equivalent ratio is similar with different MSR due to the similar distribution of temperature. At 30°CA ATDC, the area of the region with equivalent ratio around 1 decreases with increased MSR. Hence, the region with higher NO_X concentration decreases.

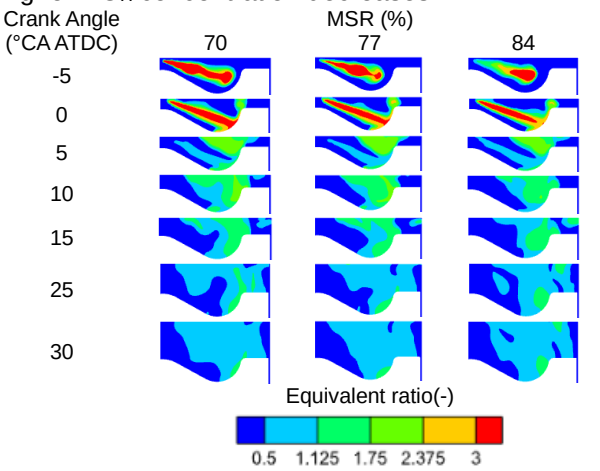

Figure 6. The effect of MSR on the distribution of equivalent ratio at 25% load

Figure 7 compares the distribution of temperature between different MSR at 25% load. At -5°CA ATDC, the area of the region with temperature higher than 1500K increases with increased MSR. According to Figure 5 and Figure 6, NO_X first occurs at the region with temperature and equivalent ratio around 2500K and 1.125, respectively. At the meantime, the high temperature region is around the fuel rich region. The combustion first occurs at the region with equivalent ratio around 1.125. At TDC, with the injection of methanol, there is a low temperature region occur in the high temperature region due to the evaporation of methanol. The distribution of high temperature region is similar to each other at different MSR at TDC due to the similar distribution of equivalent ratio (Figure 6). With the crank angle, the high temperature region shrinks gradually due to the consumption of fuel. At the 30°CA ATDC, the area of high temperature region decreases with increased MSR. It means the high temperature duration reduces with increased MSR at 25% load, which also leads the reduce of NO_X.

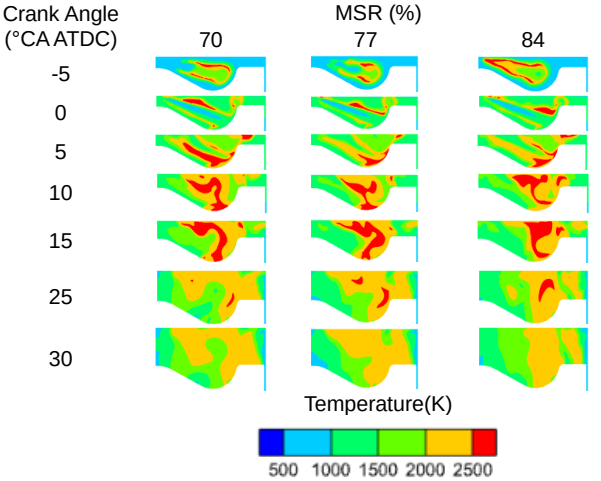

Figure 7. The effect of MSR on the distribution of temperature at 25% load

Figure 8 compares the distribution of NO_X with different MSRs at load of 100%. It can be seen that the area of distribution of NO_X first increases and then decreases with increased MSR when the crank angle is -5 °CA ATDC due to the first increased and then decreased in-cylinder temperature (Figure 12(a)). However, the mass fraction of NO_X is lower than 0.00105 at different MSRs. The distribution of NO_X extends with crank angle at different MSRs. The area of region with higher mass fraction of NO_X increases with increased MSR between combustion TDC and 5°CA ATDC due to increased area of high temperature region (Figure 9). However, the mass of diesel decreases with increased MSR. Hence, the mass of NO_X decreases with increased MSR between combustion TDC and 5°CA ATDC (Figure 16(b)). Although the in-cylinder temperature can be decreased with the increased MSR due to the evaporation of methanol. The cooling effect of methanol on in-cylinder temperature is lower than that at 25% load. The oxygenation reaction of methanol at 100% load is enhanced because of the decreased area of region with lower equivalent ratio. At 100% load, the NO_X emission first decreases and then increases with increased MSR. Hence, there is a suitable MSR for high load to obtain the lowest NO_X emission. It means that a balance between the cooling effect of methanol on in-cylinder temperature and oxygenation reaction of methanol on equivalent ratio needs to be establish to optimize the NO_X emission.

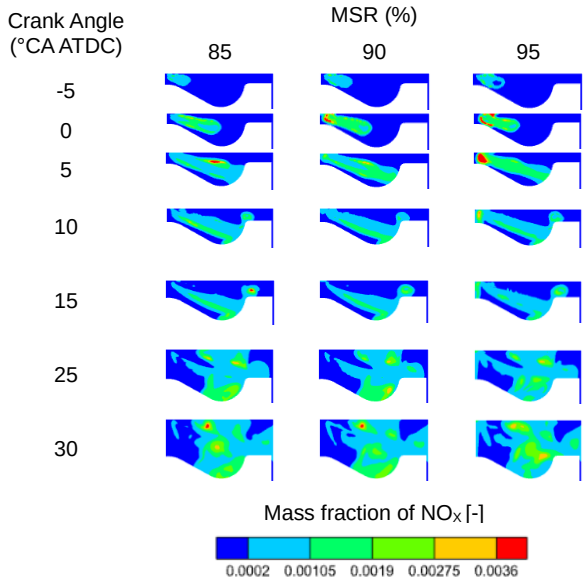

Figure 8. The effect of MSR on the distribution of NO_X at 100% load

Figure 9 shows the distribution of equivalent ratio with different MSRs at 100% load. It can be seen that spray penetration increases with the increased MSR when the crank angle is -5°CA ATDC due to increased consumption rate of diesel before methanol injection (Figure 14(b)). With the consumption of diesel, the spray penetration decreases with the increased MSR at combustion TDC. With the injection of methanol, the methanol and diesel spray impinge the piston bowl at 5°CA ATDC. The area of region with equivalent ratio higher than 3.0 decreases with increased MSR due to the enhanced evaporation effect with increased mass of methanol at 5°CA ATDC. There is a region with equivalent ratio between 1.75 and 3 around the throat of the piston bowl at all cases after 10°CA ATDC. The distance between this region and cylinder wall decreases with increased MSR. After 10 °CA ATDC, the distribution of equivalent ratio is similar with different MSRs due to the similar distribution of temperature. At 30°CA ATDC, the area of the region with equivalent ratio around 1 first decreases and then increases with increased MSR. Hence, the region with higher NO_X concentration first decreases and then increases.

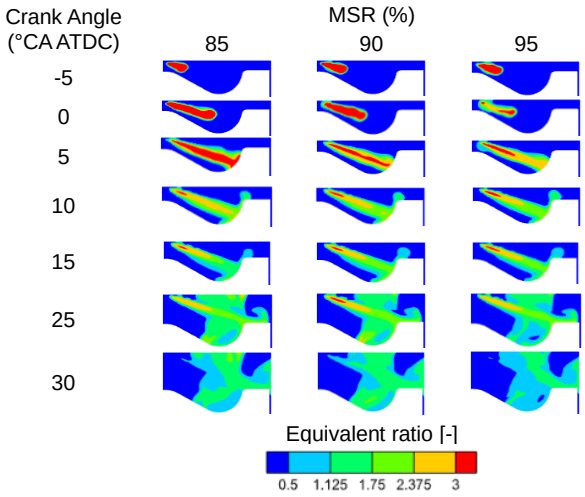

Figure 9. The effect of MSR on the distribution of equivalent ratio at 100% load

Figure 10 exhibits the distribution of temperature with different MSRs at 100% load. At -5°CA ATDC, the area of the region with temperature higher than 1500K increases with increased MSR. According to Figure 8 and Figure 9, NO_X first occurs at the region with temperature and equivalent ratio around 2000K and 1, respectively. The high temperature region is around the fuel rich region due to the evaporation of diesel. The combustion first occurs at the region with equivalent ratio around 1. At TDC, with the injection of methanol, the region with temperature at 1500K decreases with the increased MSR. However, the region with temperature higher than 2500K increases with increased MSR. The diesel flame is surrounded by the methanol spray due to the increased MSR. Hence, the diesel flame

temperature increases with increased MSR. The distribution of high temperature region is similar to each other at different MSR after TDC due to the similar distribution of equivalent ratio (Figure 9). With the crank angle, the high temperature region shrinks gradually due to the consumption of fuel. At the 30°CA ATDC, the area of high temperature region is also similar to each other at different MSRs. Compared with Figure 8 and Figure 9, the production of NO_X is mainly caused by the high oxygen concentration and the duration of high temperature.

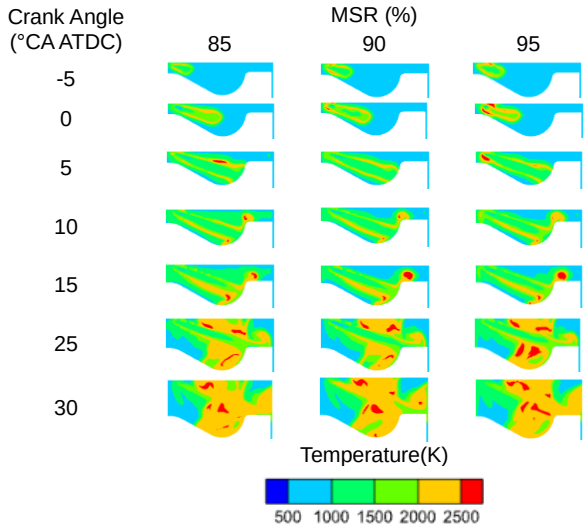

Figure 10. The effect of MSR on the distribution of temperature at 100% load

3.2 Combustion Characteristics

Figure 11 shows the in-cylinder temperature and normalized heat release rate (HRR) with different MSPs at 25% load. It can be seen from Figure 11(a) that the in-cylinder temperature increases with the movement of the piston before the injection of diesel surrogate fuel. From -45°CA ATDC to -15°CA ATDC, the in-cylinder temperature increases about 300 K with the piston movement. From -15°CA ATDC to TDC, in-cylinder temperature increases first with a higher rate caused by the combustion of diesel surrogate fuel and then with a lower rate caused by the injection of methanol into the cylinder. From TDC to 15°CA ATDC, the increase rate of in-cylinder temperature first reduces and then increases with the increased MSR due to the first reduced and then increased HRR. After -3°CA ATDC, methanol is ignited by the diesel surrogate fuel. After -3°CA ATDC, in-cylinder temperature increases with the increased HRR. After TDC, the in-cylinder temperature increases with the combustion of methanol. In the late combustion phase, the in-cylinder temperature first decreases and then increases with increased MSR at the same crank angle caused by the first decreased and then increased HRR. The peak value of the in-cylinder temperature first reduces and then increases with the increased MSR, which causes the change of combustion duration (Figure 13 (a)).

It can be seen from Figure 11 (b) that there are two HRR peaks at different MSRs. The first HRR peak is caused by the combustion of diesel surrogate fuel. The second HRR peak is resulted from the hybrid combustion process of diesel surrogate fuel and methanol. With the increased MSR, the mass of diesel surrogate fuel decreases. The ignition delay time shortens with increased MSR. Hence, the beginning time of the combustion advances with increased MSR. The equivalent mass of injected fuel per cycle is fixed at different MSRs. Hence, the CA05 advances with increased MSR due to the advanced beginning time of the combustion. The first peak value of HRR first decreases and then increases with increased MSR. From -5°CA ATDC to -2°CA ATDC, the HRR first increases and then decreases with increased MSR at the same crank angle. After -2°CA ATDC, the HRR first reduces and then increases with increased MSR. The second peak value of HRR first decreases and then increases with increased MSR. In the meantime, the late combustion phase first prolongs and then shortens, which causes the first prolonged and then shortened combustion duration.

Figure 12 shows the in-cylinder temperature and normalized HRR with different MSRs at 100% load. In Figure 12(a), similar to that at load of 25%, the in-cylinder temperature increases with the movement of the piston before the injection of diesel surrogate fuel. From -45°CA ATDC to -7°CA ATDC, the in-cylinder temperature increases about 350 K with the piston movement. From -7°CA ATDC to TDC, in-cylinder temperature increases due to the combustion of diesel surrogate fuel. From TDC to 15°CA ATDC, the increase rate of in-cylinder temperature reduces with the increased MSR due to the reduced HRR. After TDC, methanol is ignited by the diesel surrogate fuel. After TDC, in-cylinder temperature increases with the increased HRR. After TDC, the in-cylinder temperature increases with the combustion of methanol. In the late combustion phase, the in-cylinder temperature increases with increased MSR at the same crank angle caused by the increased HRR. The peak value of the in-cylinder temperature increases with the increased MSR, which causes the decrease of combustion duration (Figure 13 (b)).

It can be seen from Figure 12 (b) that there are also two HRR peaks at different MSRs like that at 25% load. The ignition delay time also shortens

with increased MSR. Hence, the beginning time of the combustion advances with increased MSR. However, the first peak value of HRR decreases with increased MSR. Hence, the CA05 retards with increased MSR. From -5°CA ATDC to TDC, the HRR decreases with increased MSR at the same crank angle. After TDC, the HRR also decreases with increased MSR due to the methanol around the diesel flame (Figure9 and Figure 10). The second peak value of HRR is equal to each other with different MSRs. There is another peak value of HRR during the late combustion phase with MSR at 90% and 95%, which can shorten the combustion duration and increase the in-cylinder temperature.

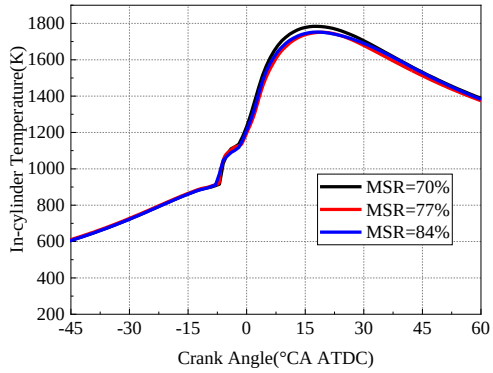

(a) In-cylinder temperature

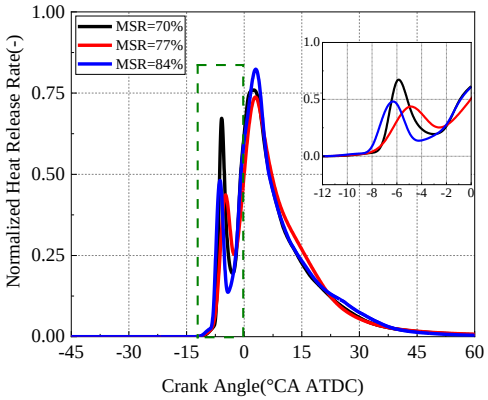

(b) Heat release rate

Figure 11. The effect of MSR on the in-cylinder temperature and heat release rate at 25% load

The combustion characteristics of the diesel-methanol dual fuel combustion mode can be described by the ignition timing (CA05), CA50 and combustion duration.

Figure 13 shows the effect of MSR on the CA05, CA50 and combustion duration with load of 25% and 100%. It can be seen from Figure 13 (a) that CA05 advances with increased MSR at load of 25% due to advanced beginning time of combustion (Figure 11(b)). CA50 retards with increases MSR due to decreased HRR. The combustion duration first prolongs and then shortens with increases MSR due to the change of HRR during the late combustion phase (Figure 11(b)). It can be seen from Figure 13 (b) that CA05 retards with increased MSR due to decreased first peak value of HRR (Figure 12(b)) at 100% load. CA50 at 100% load first retards and then advances with increases MSR due to same change of HRR. The combustion duration at 100% load shortens with increases MSR due to the increased HRR during late combustion phase (Figure 12(b)) caused by the increased flame speed of methanol.

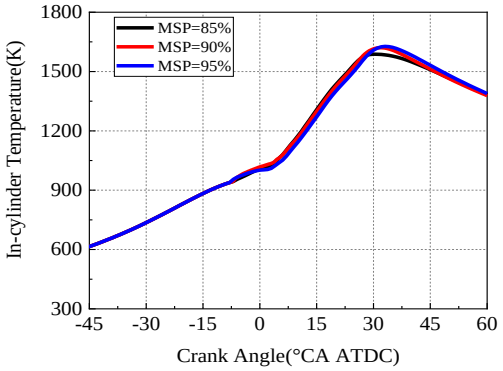

(a) In-cylinder temperature

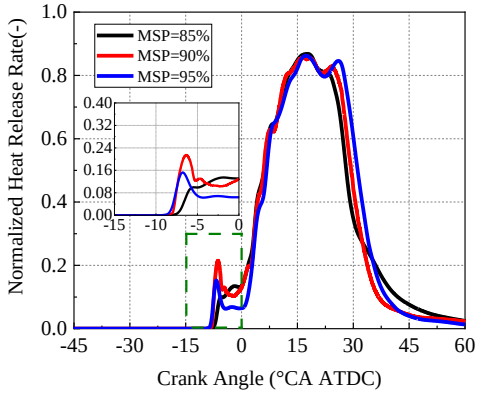

(b) Heat release rate

Figure 12. In-cylinder temperature and heat release rate with different MSRs at 100% load

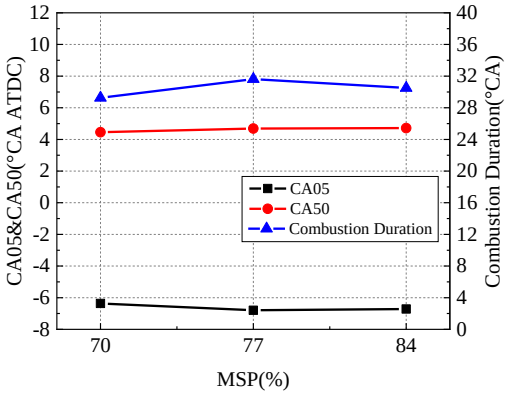

(a) 25% load

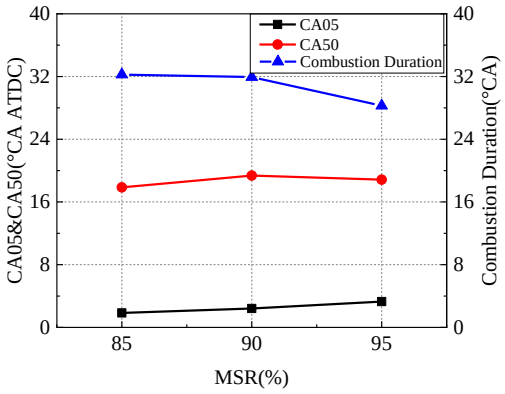

(b) 100% load

Figure 13. The effect of MSR on the CA05, CA50 and combustion duration at 25% and 100% load

3.3 Emission Characteristics

Figure 14 shows the effect of MSR on the NO_X and soot emissions. In Figure 14, the NO_X and soot emissions are normalized by the experiment data under diesel mode. It can be seen from Figure 14(a) and Figure 14(b) that the NO_X and soot emissions under methanol mode are lower than that under diesel mode. It is because that combustion temperature can be decreased by the evaporation of methanol and there is no C-C bond in the molecular structure of methanol. At load of 25%, the NO_X emission decreases with the increased MSR, which caused by the decreased maximum value of in-cylinder temperature (Figure 11(a)). The soot emission first increases and then decreases with increased MSR due to the diesel combustion process. At load of 100%, the NO_X emission first decreases and then increases with the increased MSR, which caused by the first decreased and then increased mass of methanol around the diesel flame (Figure 9 and Figure 10). The soot emission has the same trend as the NO_X emission with increased MSR due to the diesel combustion process. It can be concluded that NO_X and soot emission can be reduced by increasing MSR at low load. However, there is a suitable MSR for high load to obtain the lowest NO_X and soot emission.

To analyze the production process of NO_X, Figure 15 shows the mass of NO_X with the crank angle at load of 25% and 100%. At 25% load, the mass of NO_X decreases with increased MSR at the same crank angle due to the evaporation of methanol. At 100% load, the mass of NO_X decreases with increased MSR at the same crank angle during the early combustion phase due to the evaporation of methanol. However, the mass of NO_X first decreases and then increased with increased MSR at the same crank angle during late combustion phase due to the increased in-cylinder temperature with MSR at 95%. It means that MSR needs to be optimized to reduce the NO_X emission.

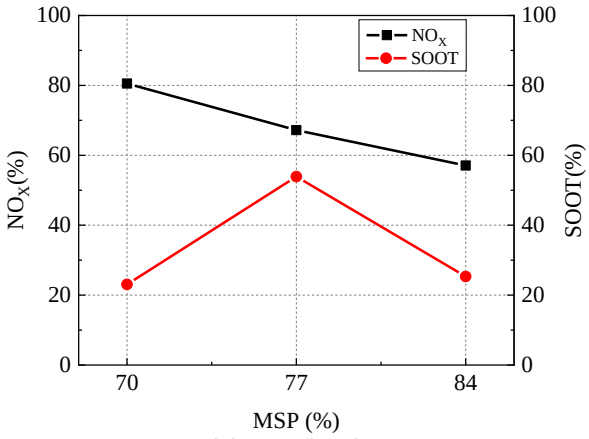

(a) 25% load

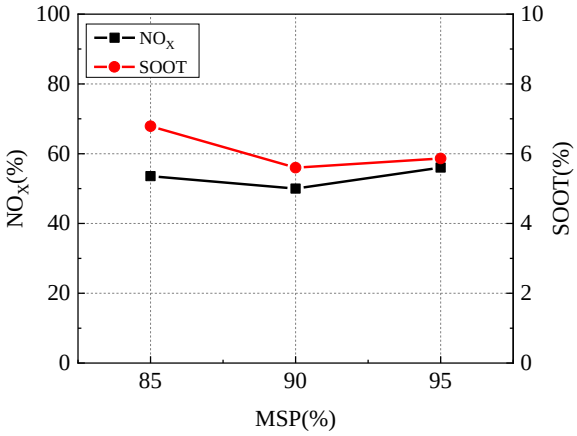

(b) 100% load

Figure 14. The emission of NO_X and soot with different MSRs at 25% and 100% load

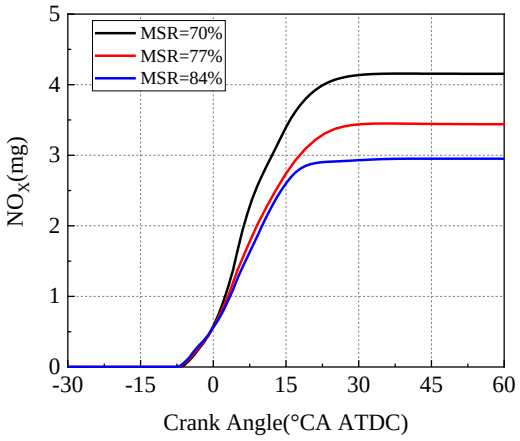

(a) 25% load

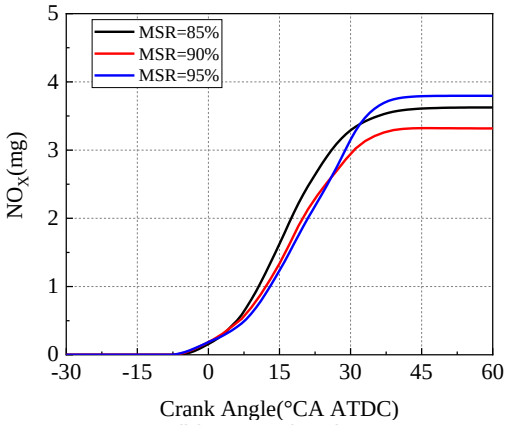

(b) 100% load

Figure 15. The effect of MSR on the mass of NO_X with the crank angle at 25% and 100% load

4 CONCLUSIONS

In this paper, diesel-methanol double direct-injection dual-fuel combustion has been simulated on a 4-stroke marine diesel engine. The effects of the MSR on the combustion and emission characteristics were simulated. The conclusions are as follows:

1. The evaporation of methanol can decrease the temperature in the cylinder, NO_X emission at 25% load. However, the enhanced oxygenation reaction of methanol at 100% increases in-cylinder temperature and NO_X emission.

2. At diesel-methanol dual-fuel combustion mode, there are two peaks on the heat release rate curves. The late combustion phase first prolongs and then shortens, which causes the first prolonged and then shortened combustion duration at 25% load. At 100% load, another peak value of HRR during the late combustion phase shortens the combustion duration and increases the in-cylinder temperature and NO_X emission.

3. The NO_X and soot emission can be reduced by increasing MSR at low load. A suitable MSR for high load is needed to obtain the lowest NO_X and soot emission. At high load, the enhanced oxygenation reaction of methanol with MSR at 95% makes the HRR increase during late combustion phase and the duration of high temperature. Hence, the NO_X emission is also higher than other cases.

5 ACKNOWLEDGMENTS

This research received funding from a government-funded project. The authors acknowledge the technical support from Shanghai Marine Diesel Engine Research Institute.

6 REFERENCES

[1] Zheng, Ye., Li, Zhenmiao., Chai, Jinlai. 2023. Progress and Prospects of International Carbon Peaking and Carbon Neutral Research –Based on Bibliometric Analysis (1991-2022), *Front. Energy Res.* 11:1121639

[2] Yao, Wang., Guo, Chi-hui., Chen, Xi-jie. et al. 2021.Carbon Peak and Carbon Neutrality in China: Goals, Implementation Path and Prospects,*China Geology* 4: 720-746.

[3] Karystinos, V., Papalambrou, G. 2023. A Phenomenological Combustion Model for Diesel-Methanol Dual-Fuel Engines, *J. Energy Resour. Technol.* 145(6): 062303.

[4] Marine Environment Protection Committee (MEPC), 73rd session, 2018.www.imo.org/en/MediaCentre/MeetingSummaries/Pages/MEPC-73rd-session.aspx.

[5] Altinkurt, MD., Merts, M., Tuner, M. et al. 2023. Effects of Split Diesel Injection Strategies on Combustion, Knocking, Cyclic Variations and Emissions of a Natural Gas-Diesel Dual Fuel Medium Speed Engine, *Fuel* 347: 128517.

[6] Ulisheney, C J., Dumitrescu, C E.2022. Effect of Gas Composition on the Performance and Emissions of a Dual-Fuel Diesel-Natural Gas Engine at Low Load Conditions,*Fuel* 324: 124531.

[7] Ma, Baodong., Yao, Anren., Yao, Chunde. et al. 2020. Exergy Loss Analysis on Diesel Methanol Dual Fuel Engine under Different Operating Parameters, *Appl. Energy* 261:114483,

[8] Yousefi, A., Guo, Hongsheng., Dev, S. et al., "A Study on Split Diesel Injection on Thermal Efficiency and Emissions of an Ammonia/Diesel Dual-Fuel Engine," *Fuel* 316:123412, 2022.

[9] Pan, Kang., Wallace, JS. 2022. Computational Studies of Hydrogen Post-Injection in Direct-Injection Natural Gas Engine, *Fuel* 323:124226.

[10] M.A. Ghadikolaei., P.K. Wong., C.S. Cheung. et al. 2021. Impact of Lower and Higher Alcohols on the Physicochemical Properties of Particulate Matter from Diesel Engines: A Review, *Renew Sustain. Energy Rev.* 143:110970.

[11] Wei, Yanju., Zhu, Zengqiang., Liu, Shenghua. et al. 2022. Investigation on Injection Strategy Affecting the Mixture Formation and Combustion of a Heavy-Duty Spark-Ignition Methanol Engine, *Fuel* 334:126680.

[12] Sayin, C., Ozsezen, A.N., Canakci, M. 2010. The Influence of Operating Parameters on the Performance and Emissions of a DI Diesel Engine Using Methanol-Blended-Diesel Fuel, *Fuel* 89: 1407–1414.

[13] Ma, Baodong., Yao, Anren., Yao, Chunde. et al. 2021. Multiple Combustion Modes Existing in the Engine Operating in Diesel Methanol Dual Fuel,*Energy* 234: 121285,

[14] Jia, Zhiqin. and Denbratt, Ingemar. 2018. Experimental Investigation into the Combustion Characteristics of a Methanol-Diesel Heavy Duty

Engine Operated in RCCI Mode, *Fuel* 226: 745-753.
[15] Yabin, D., Ossi, K., Ghulam, H. et al. 2020. High-Pressure Direct Injection of Methanol and Pilot Diesel: A Non-Premixed Dual-Fuel Engine Concept, *Fuel* 277:117932.
[16] Huang, Z., Lu, H., Jiang, D. et al. 2004.Combustion Behaviors of a Compression-Ignition Engine Fueled with Diesel/Methanol Blends under Various Fuel Delivery Advance Angles, *Bioresource Tech.* 95(3): 331-341,
[17] Wei, Lijiang., Yao, Chunde., Wang, Quangang. et al. 2015. Combustion and Emission Characteristics of a Turbocharged Diesel Engine Using High Premixed Ratio of Methanol and Diesel Fuel, *Fuel* 140:156–163.
[18] Wang, Bin., Yao, Anren., Chen, Chao. et al. 2019.Strategy of Improving Fuel Consumption and Reducing Emission at Low Load in a Diesel Methanol Dual Fuel Engine, *Fuel* 254:115660.
[19] Qu, Guofan., Yao, Anren., Chen, Chao. et al. 2021. Effect of EGR Strategy on Combustion and Emission of DMDF Engine for Meeting China VI Emission Legislation, *Fuel* 299:120879.
[20] MAN L35/44DF Project Guide, 2022.
[21] Wärtsilä W3 Project Guide, 2022.
[22] Yao, Chunde., Pan, Wang., Yao, Anren.2017. Methanol Fumigation in Compression-Ignition Engines: A Critical Review of Recent Academic and Technological Developments, *Fuel* 209:713-732.
[23] Han, Dong., Lyu, DL., Sun, Zijian. et al. 2022.On Knocking Combustion Development of Oxygenated Gasoline Fuels in a Cooperative Fuel Research Engine, *Int. J. Engine Res.*
[24] Li, Zhiyong., Wang, Yang., Yin, Zibin. et al. 2021. Parametric Study of a Single-Channel Diesel/Methanol Dual-Fuel Injector on a Diesel Engine Fueled with Directly Injected Methanol and Pilot Diesel, *Fuel* 302:121156.